

Aerosol influence on mixed-phase clouds in CAM-Oslo

Trude Storelvmo

Department of Geosciences, University of Oslo, Oslo, Norway

Jón Egill Kristjánsson

Department of Geosciences, University of Oslo, Oslo, Norway

Ulrike Lohmann

Institute for Atmospheric and Climate Science, ETH Zurich, Zurich, Switzerland

Corresponding author address: Trude Storelvmo, Department of Geosciences, P.O.Box 1022 Blindern, 0315 Oslo, Norway.

E-mail: trude.storelvmo@geo.uio.no

ABSTRACT

A new treatment of mixed-phase cloud microphysics has been implemented in the general circulation model CAM-Oslo, which combines the NCAR CAM2.0.1 and a detailed aerosol module. The new treatment takes into account the aerosol influence on ice phase initiation in stratiform clouds with temperatures between 0°C and -40°C. Both supersaturation and cloud ice fraction, i.e. the fraction of cloud ice compared to the total cloud water in a given grid box, are now determined based on a physical reasoning by which not only temperature but also the ambient aerosol concentration plays a role. Included in the improved microphysics treatment is also a continuity equation for ice crystal number concentration. Ice crystal sources are heterogeneous and homogeneous freezing processes and ice multiplication. Sink terms are collection processes and precipitation formation, melting and sublimation. Instead of using an idealized ice nuclei concentration for the heterogeneous freezing processes, a common approach in global models, the freezing processes are here dependent on the ability of the ambient aerosols to act as ice nuclei. Additionally, the processes are dependent on the cloud droplet number concentration and hence the aerosols' ability to act as cloud condensation nuclei. Sensitivity simulations based on the new microphysical treatment of mixed-phase clouds are presented for both pre-industrial and present-day aerosol emissions. Freezing efficiency is found to be highly sensitive to the amount of sulphuric acid available for IN coating. In the simulations, the interaction of anthropogenic aerosols and freezing mechanisms causes a warming of the earth-atmosphere system, counteracting the cooling effect of aerosols influencing warm clouds. We find that this reduction of the total aerosol indirect effect amounts to 50-90%. However, many microphysical processes in mixed-phase clouds are still poorly understood and the results must be interpreted with that in mind.

1. Introduction

a. Aerosol effects on warm and cold clouds

The importance of understanding aerosols' influence on climate, not only directly but also through their interaction with clouds has been pointed out in several studies in recent years (Hansen et al., 2002 and Kerr, 2005). The uncertainty associated with the impact of anthropogenic aerosols on clouds is a major contributor to the spread in future climate projections, as the estimates of this aerosol indirect effect (AIE) in different global climate models (GCMs) vary significantly (Andreae et al., 2005).

A multitude of studies have been carried out in recent years, investigating aerosol effects on warm clouds in numerical models on different scales. In most (if not all) of these studies, the aerosol indirect effect on warm clouds was found to represent a cooling in the present climate (Takemura et al., 2005, Rotstayn and Liu, 2003, Menon et al, 2002, Lohmann et al., 2000, Kristjánsson, 2002 and Storelvmo et al., 2006a). The cooling is caused by an increase in cloud albedo through the *Twomey* (Twomey, 1977) and *Albrecht* (Albrecht, 1989) effects. The Twomey effect refers to the process through which anthropogenic aerosols lead to an increase in cloud droplet number concentration and therefore smaller droplets (if cloud water remains unchanged). This process is also referred to as the *radius effect*. The Albrecht effect refers to the increase in cloud cover, thickness and/or lifetime associated with the less efficient precipitation release as droplets become smaller. This effect is sometimes also referred to as the *lifetime effect*.

Although unresolved problems still exist, it is fair to say that the understanding of the aerosol indirect effect on warm clouds has improved as more effort has been put into

investigating this topic, in many cases combining observations and models (Quaas et al., 2006 and Storelvmo et al., 2006b). On the other hand, the general understanding of the aerosol indirect effect on cold clouds is still fairly poor (Lohmann and Feichter, 2005), and the current ability to describe cold clouds in global models is very limited. This is partly due to the even higher degree of complexity introduced as soon as the ice phase occurs in a cloud, but possibly also because the availability of high quality observational data has so far been limited.

First of all, determining the ice fraction (cloud ice divided by total cloud water) of a cloud is fundamental for calculations of its radiative properties, but not at all straightforward. Secondly, determining the ice water content and the ice crystal number concentration correctly is extremely important and equally challenging. Finally, determining the sizes and shapes of ice crystals is crucial for determining the radiative properties of ice-containing clouds. In contrast to cloud droplets, ice crystals are hardly ever spherical, complicating this matter. All the parameters mentioned above are to some extent influenced by aerosols through various processes, many of which are not well understood (Pruppacher and Klett, 1997).

A complicating factor associated with cold clouds is the number of different freezing processes that can initiate cloud ice formation or cloud glaciation. While warm clouds always form by water vapor condensing onto cloud condensation nuclei (CCN), the situation is far more complex in the case of ice clouds. Ice crystals can form through freezing of cloud droplets, without the aid of freezing nuclei facilitating the phase transition. This homogeneous freezing is limited to temperatures below approximately -40°C (Pruppacher and Klett, 1997). For warmer temperatures, ice clouds are formed through various heterogeneous freezing processes, meaning that so called ice nuclei (IN) facilitate the phase

transitions from vapor or liquid water to ice. The different heterogeneous freezing mechanisms (contact, immersion, condensation and deposition freezing) are described in detail in e.g. Vali (1985). Natural IN are typically insoluble dust aerosols and certain biogenic aerosols (Pruppacher and Klett, 1997). Aerosols with crystalline structures seem to be particularly suitable for ice nucleation. Soot particles in the atmosphere are considered to be almost entirely of anthropogenic origin, and were found to be efficient IN via the contact freezing mode in a laboratory study by Gorbunov et al. (2001). They studied the ice nucleating ability of generated small soot particles with different surface properties, and found them to be relatively potent ice nucleators. More recently, Dymarska et al. (2006) presented results apparently contradicting these findings. However, this study was carried out for deposition freezing, whereas the freezing observed by Gorbunov et al. (2001) has until recently been interpreted as contact freezing. Currently, it is under debate whether this was actually the freezing mechanism observed. One must also keep in mind that the relevance of the findings of Gorbunov et al. (2001) depends on the extent to which the generated soot particles are representative for soot particles found in the atmosphere.

Yet another challenge introduced when considering the formation of cold clouds is the so called *Bergeron-Findeisen process* in which ice crystals, once formed, grow rapidly at the expense of the surrounding cloud droplets due to the difference in saturation vapor pressure over water compared to that over ice.

Finally, secondary ice formation processes are thought to influence ice crystal number concentrations significantly, especially in certain temperature intervals. One example is the so called Hallett-Mossop process (Hallett and Mossop, 1974), which refers to the ice splintering occurring as droplets impact upon ice crystals during riming. However, several other secondary ice production theories exist (e.g. the fragmentation of dendritic ice crystals

typically forming at temperatures from -16°C to -12°C). Unfortunately, these mechanisms are not well understood at all, and the only such process so far attempted parameterized for model studies is the Hallett-Mossop process.

b. Modeling aerosol effects on mixed-phase and cirrus clouds

In many state-of-the-art GCMs, the cloud ice fraction (f_{ice}) is determined using a highly simplified approach. In these models, ice fraction is simply a function of one parameter only, namely the temperature of the given model grid box. Conversely, in the real atmosphere, the cloud ice fraction is determined by a number of parameters, important ones being supersaturation, atmospheric stability, ambient aerosol concentrations, cloud age and temperature. An attempt to take more of these parameters into account when determining f_{ice} has been developed by Lohmann(2002) for the ECHAM4 GCM. This study was one of the first addressing aerosol indirect effects associated with mixed-phase clouds. It has been shown experimentally (Pitter and Pruppacher, 1973) that when cloud droplets become smaller as a result of increased cloud droplet number concentration (CDNC), for example as a result of anthropogenic aerosols, they require lower temperatures in order to freeze. On the other hand, it could be argued that an increase in CDNC might increase the probability of freezing (Lohmann, 2002). Clearly, these two effects counteract each other, and the net radiative effect was found to be small in Lohmann et al. (2000). In addition to the two effects mentioned, aerosols may also influence cold clouds by acting as IN in heterogeneous freezing processes. In Lohmann (2002) a prognostic treatment of ice crystal number concentration was employed to study the anthropogenic aerosol effect on contact freezing. Other heterogeneous freezing processes than contact freezing were parameterized independently of the IN

concentrations predicted by the model and aerosols were not allowed to influence freezing processes at temperatures below -35°C . Nevertheless, a potentially high sensitivity to anthropogenic aerosols was found.

At temperatures below -35°C , the rate of ice crystal formation was determined based on saturation adjustment with respect to ice and the parameterization of ice crystal size developed by Ou and Liou (1995). The latter expresses ice crystal effective radius as a function of temperature. Similar relationships have been developed by Kristjánsson et al. (2000), Ivanonva et al. (2001) and Boudala et al. (2002). Unfortunately, these relationships deviate quite substantially from each other for certain temperature intervals. As these empirical relationships stem from field campaigns in different environments, this is not surprising and points out the need for more observations. Ideally, ice crystal sizes could be determined as long as ice crystal number concentration (ICNC) and ice water content (IWC) are known. With prognostic model equations for ice crystal number concentrations, this can be achieved. However, such an approach is not as straightforward for ice clouds as it is for liquid clouds. Whereas cloud droplets are always spherical, a wide range of ice crystal shapes (McFarquhar and Heymsfield, 1996) have been observed. Consequently, one must know or make assumptions on crystal shape before an effective size can be calculated.

In more recent model studies by Diehl and Wurzler (2004) and Diehl et al. (2006), the effectiveness of dust and black carbon (BC) aerosols as contact and immersion freezing IN was parameterized based on laboratory studies. These parameterizations were implemented in the ECHAM4 GCM by Lohmann and Diehl (2006). This was the first global study taking the chemical composition of the IN into account, and a significant sensitivity to this parameter was found in the net radiation at the top of the atmosphere (TOA). This study focused on mixed-phase clouds, i.e. clouds at temperatures between 0°C and approximately -35°C .

A global study of cirrus cloud formation (i.e. formation of pure ice clouds at temperatures below -38°C) was carried out by Lohmann and Kärcher (2002), abandoning the saturation adjustment approach used by most models. Homogeneous freezing processes were reported to be controlled primarily by vertical velocity and temperature, while details of the aerosol size distributions were less important. Previously, the strong dependence of cirrus microphysical properties on updraft velocity was also shown by e.g. Jensen et al. (1994). Aircraft data suggests that freezing in mid-latitude cirrus could be initiated at ice saturation ratios lower than those required for homogeneous freezing (Heymsfield et al., 1998). DeMott et al. (1997) studied cirrus cloud formation in an adiabatic parcel model, and found that heterogeneous freezing processes can significantly influence ice crystal formation at vertical updraft velocities lower than approximately 20 cm/s. At higher updraft velocities, they found homogeneous freezing to be the dominating mechanism. This sensitivity to updraft velocities was confirmed in a parcel model study by Kärcher and Lohmann (2003). More recently, Kärcher et al. (2006) took into account the competition between homogeneous and heterogeneous freezing processes in a parameterization suitable for GCM simulations. By allowing for this competition, they found that much stronger indirect aerosol effects on cirrus clouds are possible.

The purpose of this study is twofold: Firstly, we present the first version of a parameterization of aerosol mixed-phase cloud interactions, which builds on the previous approach for warm clouds (Storelvmo et al., 2006a). Secondly, this parameterization is tested in a set of experiments which quantify the aerosol indirect effect of mixed-phase clouds. The study is motivated by the limited understanding of how mixed-phase clouds are influenced by aerosols, and the current scarcity of global estimates of this effect. The parameterization employed is similar to that used in Lohmann and Diehl (2006), and has been implemented in

the CAM-Oslo GCM, which is a modified version of the NCAR CAM-2.0.1 (<http://www.cesm.ucar.edu/models>). CAM-Oslo and its framework for calculations of aerosol effects on warm clouds were previously presented in detail in Storelvmo et al. (2006a). The corresponding framework for aerosol effects on mixed-phase clouds will be presented in the following section, and the main results will be presented in Section 3. Section 3 also contains a discussion of the results in light of available observations and results from other model studies. In section 4 we present the results of three sensitivity tests, where we have varied uncertain parameters in the new parameterization, to get an indication of the robustness of the results. Finally, Section 5 contains a conclusion and suggestions of steps that could be taken to improve the current framework in the future.

2. CAM-Oslo and the new framework for calculations of AIE on mixed-phase clouds

a. CAM-Oslo

CAM-Oslo is an extended version of the National Center for Atmospheric Research (NCAR) Community Atmosphere Model Version 2.0.1 (CAM2.0.1). CAM-Oslo is based on the primitive equations solved for 26 vertical levels ranging from sea level to approximately 3.5 hPa. For this study, we ran the model simulations with an Eulerian dynamical core at T42 spectral truncation, corresponding to a horizontal grid spacing of $2.8^\circ \times 2.8^\circ$ and a dynamical timestep of 20 minutes. The process of deep convection is treated with a parameterization scheme of Zhang and McFarlane (1995). The scheme is based on a convective plume

ensemble approach, i.e. it assumes that whenever the lower troposphere is conditionally unstable an ensemble of convective scale updrafts may exist. The parameterization of non-convective cloud processes follows Rasch and Kristjánsson (1998). This cloud microphysics scheme carries water vapor and cloud water (i.e. the sum of liquid and ice condensates) as prognostic variables. Stratiform clouds are assumed to be sufficiently short-lived that resolved advection has little influence upon them, while convective and turbulent processes may affect them. This is justified by the fact that over the lifetime of a typical cloud in the model, large scale advection would not have a strong influence, while parameterized smaller scale mechanisms would. The fractional cloud cover is determined based on the relative humidity and (a variable describing) vertical static stability. A maximum/random cloud overlap approach (Collins, 2001) is taken for radiation interactions with clouds, which is otherwise described by Slingo (1989) and Kiehl et al. (1994) for water clouds and by Ebert and Curry(1992) for ice clouds. Previous extensions to the host model (i.e. CAM2.0.1) to form CAM-Oslo were implementations of: i) An aerosol lifecycle module (Iversen and Seland, 2002), ii) An aerosol size distribution module (Kirkevåg et al., 2005), iii) A module for calculations of AIE of warm clouds (Storelvmo et al., 2006a). The aerosol lifecycle module predicts mass mixing ratios for sulfate and carbonaceous aerosols based on AEROCOM (<http://nansen.ipsl.jussieu.fr/AEROCOM>) emissions. Gas phase and aqueous chemistry, coagulation and dry and wet deposition are treated by the module. Sea salt and mineral dust aerosols are treated as background aerosols in the current model setup, meaning that their size distributions are prescribed according to surface properties and latitude. In the size distribution module, the sulfate, BC and OC aerosol concentrations are combined with the background aerosol (Kirkevåg and Iversen, 2002). The background aerosol size distribution is described by two lognormal mineral dust modes (accumulation and coarse

mode) and three lognormal sea salt modes (fine, accumulation and coarse modes). Both the aerosol size distribution and composition are modified as sulfate, OC and BC are internally mixed with the background aerosol. However, sulfate, BC and OC may also be externally mixed with the background in lognormal nucleation modes. All species except externally mixed BC can act as CCN, as we assume even mineral dust to be slightly soluble according to Ghan et al. (2001).

b. New parameterization

We now describe the new module for calculations of AIE on mixed-phase clouds, which also ensures that cloud formation is treated in a more physical manner than previously. Firstly, in the new framework, cloud condensate is split up, so that cloud liquid water and cloud ice water are now two separate prognostic variables. The host model does not treat ice saturation separately, but rather approximates it as a weighted average of the saturation ratios with respect to ice and water between 0°C and -20°C. At temperatures below -20°C saturation with respect to ice is assumed. In the new framework, a newly formed cloud at temperatures above -40°C is assumed to be saturated with respect to water. This is in better agreement with the observations reported by Korolev and Isaac (2006). However, as heterogeneous freezing processes form sufficient ice crystals to allow the Bergeron-Findeisen process to become efficient, supersaturation with respect to ice is assumed. Currently, if a critical cloud ice mixing ratio of $5 \cdot 10^{-6}$ kg/kg is reached by heterogeneous freezing processes, this transition occurs in the model. This is an attempt to account for the Bergeron-Findeisen process in the

model, and is an aspect of the parameterization that we hope to improve in the future, ideally based on laboratory or in situ measurements.

The calculation of cloud ice fraction is also improved in the new framework. In the host model, ice fraction increases linearly from 0 to 1 over the temperature range from 0°C to -20°C. In the new framework, the ice fraction is calculated as follows:

$$f_{ice} = \frac{q_i}{q_i + q_l} \quad (1)$$

where q_i and q_l are cloud ice water mixing ratio and cloud liquid water mixing ratio, respectively. Conservation equations for q_l and q_i are:

$$\frac{dq_l}{dt} = A_{q_l} + Cond - (PWAUT + PSACW + PRACW) - frz_{imm} - frz_{con} - frz_{q,hom} + mlt_q - E \quad (2)$$

$$\frac{dq_i}{dt} = A_{q_i} + Dep - (PSAUT + PSACI) + frz_{imm} + frz_{con} + frz_{q,hom} - mlt_q - subl \quad (3)$$

where (2) is an extension of the corresponding equation in Rasch and Kristjansson (1998), while (3) is a new equation. The different terms on the right hand side are explained below. In addition, a prognostic equation for ice crystal number concentration is part of the new framework:

$$\frac{dN_i}{dt} = A_{N_i} + \frac{N_i}{q_i} (-PSAUT - PSACI - subl) + \frac{N_i}{q_l} (frz_{imm} + frz_{con}) + frz_{N,hom} - mlt_N - selfc_i + mult \quad (4)$$

Cond: Rate of condensation (vapor to cloud liquid water) $(\text{kg}(\text{kg}\cdot\text{s}))^{-1}$
Dep: Rate of water deposition (vapor to cloud ice) $(\text{kg}(\text{kg}\cdot\text{s}))^{-1}$
N_i: Ice crystal number concentration (m^{-3})
A_{qx}: Transport (convection and turbulence) $(\text{kg}(\text{kg}\cdot\text{s})^{-1})$
A_{Nx}: Transport (convection and turbulence) $(\text{m}^{-3}\text{s}^{-1})$
PSAUT: Rate of autoconversion of ice condensate to snow $(\text{kg}(\text{kg}\cdot\text{s})^{-1})$
PWAUT: Rate of autoconversion of liquid condensate to rain $(\text{kg}(\text{kg}\cdot\text{s})^{-1})$
PSACI: Rate of snow accreting ice $(\text{kg}(\text{kg}\cdot\text{s})^{-1})$
PSACW: Rate of snow accreting water $(\text{kg}(\text{kg}\cdot\text{s})^{-1})$
PRACW: Rate of rain accreting water $(\text{kg}(\text{kg}\cdot\text{s})^{-1})$
frz_{imm}: Rate of immersion freezing $(\text{kg}(\text{kg}\cdot\text{s})^{-1})$
frz_{con}: Rate of contact freezing $(\text{kg}(\text{kg}\cdot\text{s})^{-1})$
frz_{q hom}: Rate of homogeneous freezing to form cloud ice $(\text{kg}(\text{kg}\cdot\text{s})^{-1})$
frz_{N hom}: Rate of homogeneous freezing to form ice crystals $(\text{m}^{-3}\text{s}^{-1})$
subl: Rate of sublimation of cloud ice $(\text{kg}(\text{kg}\cdot\text{s})^{-1})$
mlt_q: Rate of melting of cloud ice $(\text{kg}(\text{kg}\cdot\text{s})^{-1})$
mlt_N: Rate of melting of ice crystals $(\text{m}^{-3}\text{s}^{-1})$
selfc_i: Self-collection of ice crystals $(\text{m}^{-3}\text{s}^{-1})$
mult: Ice multiplication (Hallett-Mossop process) $(\text{m}^{-3}\text{s}^{-1})$
E: Rate of evaporation of cloud liquid water $(\text{kg}(\text{kg}\cdot\text{s})^{-1})$

A corresponding prognostic equation for cloud droplet number concentration, previously described in Storelvmo et al. (2006a), is modified here so that the loss of droplets due to freezing processes is now explicitly accounted for:

$$\frac{dN_l}{dt} = A_{N_l} + \text{nucl} - \frac{N_l}{q_l} (\text{PSAUT} + \text{PSACI} + E + \text{frz}_{\text{imm}} + \text{frz}_{\text{con}}) - \text{frz}_{N,\text{hom}} + \text{mlt}_{N_l} - \text{selfc}_l \quad (5)$$

N_i : Cloud droplet number concentration in m^{-3}

$selfc_i$: Self-collection of cloud droplets ($m^{-3}s^{-1}$)

$nucl$: Cloud droplet nucleation ($m^{-3}s^{-1}$)

The source term in this equation ($nucl$) is based on the cloud droplet activation scheme of Abdul-Razzak and Ghan (2000). In equations (2) and (3), the condensation and deposition terms are determined by a saturation adjustment scheme presented in detail in Rasch and Kristjánsson (1998). The saturation adjustment approach is not suitable for cirrus cloud formation due to the high supersaturations observed for such clouds (e.g. Peter et al., 2006), while for mixed-phase clouds it is an acceptable approximation. For newly formed clouds, the adjustment is carried out with respect to supersaturation over water for temperatures above -40°C . For temperatures at which homogeneous freezing processes can occur ($T < -40^\circ\text{C}$ here), ice saturation is assumed and ice crystal formation is calculated as in Lohmann and Diehl (2006). Hence, the homogeneous nucleation rate of ice crystals is determined by the following equation:

$$frz_{\text{hom}} = \frac{3\rho_0 q_i^{\text{new}}}{4\pi\rho_i r_i^3} \times \frac{1}{\Delta t} \quad (6)$$

where ρ_0 is the air density in kg/m^3 , q_i^{new} is the newly formed or detrained ice mass mixing ratio in kg/kg , ρ_i is the density of bulk ice (kg/m^3) and Δt is the length of a timestep (1200 s).

r_{iv} is the mean volume radius of the ice crystals, parameterized as a function of temperature as explained in Lohmann (2002). Applying a saturation adjustment scheme for cirrus clouds is clearly a simplification, as high supersaturations with respect to ice are often observed at these temperatures. The ice multiplication term is calculated as in Levkov et al. (1992), and occurs only at temperatures between -3°C and -8°C in the presence of relatively large droplets. It is given by the following equation:

$$mult = \begin{cases} K(1 - f_{25}) \cdot J; T \in (265 \text{ K}, 270 \text{ K}) \\ 0; otherwise \end{cases} \quad (7)$$

where T is temperature in K, K is a temperature dependent coefficient, f_{25} is the fraction of cloud droplets smaller than $25 \mu\text{m}$ in diameter and J is the collision-rate between snow crystals and cloud droplets greater than $25 \mu\text{m}$ in diameter. For further details on J , see Levkov et al. (1992).

The precipitation terms in equations (2)-(4) (PWAUT, PSAUT, PRACW, PSACW and PSACI) are identical to those of Rasch and Kristjánsson (1998). If a cloud exists in a sub-saturated grid box, cloud particles are evaporated or sublimated until saturation is reached or until the entire cloud has dissipated. In a mixed-phase cloud, all liquid droplets will evaporate before the ice crystals start to sublimate, due to the difference in saturation pressure between the two water phases. Melting occurs when ice crystals are present in a grid box with temperatures above 0°C . The heterogeneous freezing terms in equations (3) and (4) are calculated based on the parameterizations developed by Diehl and Wurzler (2004) and Diehl et al. (2006), implemented as in Lohmann and Diehl (2006). The immersion and contact nuclei concentrations are obtained by multiplying mineral dust and black carbon concentrations with their respective temperature-dependent freezing efficiencies. The freezing efficiencies are independent of IN sizes, which is a possible weakness of this

parameterization. According to classical heterogeneous nucleation theory, the heterogeneous nucleation rate is independent of IN size. Still, in a laboratory study by Hung et al. (2003) a weak dependency on IN size was found for the heterogeneous freezing rate. They suggested that an alternative theory taking so called “active sites” into account is required to explain their results. Additionally, IN measurements from the SUCCESS (Subsonic Aircraft: Contrail and cloud effect special study) campaign showed very low IN concentrations for IN radii below 100 nm, indicating the existence of a lower size limit for IN (Chen et al., 1998). However, the findings of Sax and Goldsmith (1972) showing the efficiency of aitken mode (~10 nm) AgI particles as contact IN contradict such a lower size limit.

3. Results from reference simulations

a. Simulation setup

For all model setups presented in this section and the following, we have performed two model simulations: one with aerosol emissions corresponding to present day (PD) conditions (AEROCOM B), and the other with pre-industrial (PI) emissions (AEROCOM PRE). The anthropogenic influence on various model parameters is calculated as the difference between the PD and PI run (PD minus PI) for the given parameters. Each model simulation is run for 5 years after a model spin-up of one month. All figures show 5-year averages. Table 1 provides a short description of the two model setups discussed in this section and the 3 sensitivity studies presented in Section 4. In Table 2, cloud microphysical and radiative properties averaged globally and over 5 years are given for the five model setups. Anthropogenic changes for these parameters are also given in all five cases.

In the reference run (Simulation AIE_ref), we made a major simplification by assuming that all dust and soot aerosols may act as IN both in the immersion and contact freezing mode (however, they are still multiplied by their respective freezing efficiencies). This is not realistic, as a requirement for contact IN is that they are practically insoluble whereas immersion IN need to be partly soluble or coated by a soluble material in order to become immersed in a cloud droplet. Figures 1a-c show the zonal mean concentrations of dust and BC aerosols for PD and PI conditions. Evident from the figures is the high mineral dust number concentration in CAM-Oslo, compared to for example that of ECHAM4, presented in Lohmann and Diehl (2006). As the assumption that all BC and mineral aerosols may act as both immersion and contact IN may not be a good one, the reference simulation is not necessarily the most realistic one. Rather, it is a simple starting point for the three different and possibly more realistic sensitivity tests that will be presented in the following section. Yet another simplification is made by assuming that all mineral dust aerosols consist of montmorillonite, which is a type of dust particularly suitable for ice nucleation. This is justified by a modeling study by Hoose et al. (2007), where the assumption that all dust is montmorillonite gave similar results to using realistic dust mineralogy. One class of very efficient IN is entirely left out, namely biogenic particles like bacteria, algae, spores etc. According to Jaenicke (2005), such aerosols constitute a significant fraction of the total aerosol mass in many areas. Unfortunately, CAM-Oslo currently does not carry such aerosols, and neither does any other GCM to our knowledge. We will discuss this issue further in Section 5. In the following subsection we will compare the results from the reference run with a simulation in which the new framework is excluded, and where aerosols are only allowed to influence liquid clouds (Simulation AIE_liq).

b. Aerosol influence on warm and cold clouds

In order to separate the effects of anthropogenic aerosols on ice crystal production, we have carried out a simulation AIE_liq, in which aerosols do not influence the clouds in any other way than through acting as CCN. This simulation corresponds most closely to the previous model configuration of Storelvmo et al. (2006a). Hence, only aerosol effects on warm clouds are taken into account in this simulation, while the cloud ice fraction is determined by temperature only (being 0 at 0°C and 1 at -20°C). By comparing the AIE in this simulation with that in AIE_ref, an estimate of the “cloud glaciation effect” can be made. The framework for calculation of aerosol effects on warm clouds is similar to that of Storelvmo et al. (2006a) (hereafter S2006), with one important difference: While the AIE was calculated off-line in S2006 (meaning that aerosol effects on clouds were not allowed to influence the model meteorology), the AIE on warm clouds is here calculated on-line. Another more subtle difference is that here dust aerosols are assumed to be practically insoluble, whereas in the control run of S2006 they were assumed to be slightly soluble (solubility of 0.013) and therefore contributing to the CCN concentration.

The net cloud forcing (NCF) is defined as the sum of the shortwave- and longwave cloud forcings (SWCF and LWCF, respectively), which are given in Table 2. The difference in NCF between the PD and PI simulation at the TOA in the AIE_liq case is -0.49 W/m^2 . This is slightly higher than in the control run in S2006 (-0.3 W/m^2), which is partly due to the reduction in dust aerosol solubility leading to fewer natural CCN. This also indicates that in CAM-Oslo, the impact of warm cloud AIE on the model meteorology is relatively small, at least when measured in radiative fluxes at the TOA averaged over a sufficient time period. The reduction in NCF at the TOA when anthropogenic aerosols are introduced is caused by a

reduction in effective radius of $-0.44 \mu\text{m}$ and an increase in Liquid Water Path (LWP) of 0.87 g/m^2 . Both changes lead to an increase in cloud albedo and hence more solar radiation reflected back to space. Changes in Ice Water Path (IWP) and Total Cloud Cover (TCC) are negative, but very small.

In the new framework clouds may contain liquid water at temperatures as low as -40°C , consistently with experimental data on the homogeneous freezing threshold. However, warmer homogeneous freezing thresholds as high as -35°C also appear in the literature. This threshold is highly dependent on droplets sizes, and for our purpose a -40°C threshold seems reasonable. Our results appear to be relatively insensitive to varying the threshold within the range found in the literature. This is also in agreement with occasional reports of aircraft icing and field campaigns reporting liquid water at such temperatures (Intrieri et al. 2002). Conversely, if sufficient IN are present, freezing may be efficient enough for clouds to become completely glaciated even at temperatures close to 0°C , as observed by e.g. Sassen et al. (2003) in the CRYSTAL-FACE campaign. Cloud ice fractions for AIE_ref and AIE_liq (PD simulations) as functions of pressure are presented in Figure 2. Clearly, the new framework (AIE_ref) allows more ice formation in low (i.e. warm) clouds, and also enables the existence of liquid water at levels higher (i.e. colder) than in AIE_liq (which corresponds to the host model, CAM2.0.1, approach in this respect). Allowing liquid water at temperatures down to -40°C rather than -20°C leads to a significantly higher LWP in the AIE_ref case compared to AIE_liq. Additionally, as precipitation release via the ice phase is more efficient for pure ice clouds than for mixed phase clouds in the model (true for all simulations), the IWP also increases, as the temperature interval in which mixed-phase clouds may exist is wider.

As anthropogenic BC aerosols increase the number concentration of IN in the present-day case, heterogeneous freezing processes are more efficient in the AIE_ref PD simulation than in the PI one. Consequently, the difference in LWP between the PD and the PI runs is now negative, although small (Table 2). Hence, the Albrecht effect is completely cancelled in AIE_ref by the so-called aerosol glaciation effect. As a result of the more efficient heterogeneous freezing, IWP increases as anthropogenic aerosols are introduced. The increase is relatively small, as the precipitation release through the ice phase is more efficient than for clouds containing water droplets. Total cloud cover is slightly higher in the PD than in the PI case. The anthropogenic changes in cloud microphysics discussed above result in a smaller reduction in the NCF at the TOA than in the AIE_liq runs, being only -0.07 W/m^2 in this simulation. It corresponds to a reduction in the total AIE compared to AIE_liq by almost 90%, leaving the total AIE practically negligible compared to for example the positive forcing associated with the anthropogenic increase in greenhouse gases. By total AIE we refer to all effects that are caused by anthropogenic aerosols acting as CCN or IN. Hence, semi-direct effects are not included. As mentioned already this simulation is not necessarily the most realistic one carried out in this study. The three sensitivity studies presented in the following section are attempts to correct for aspects that may be unrealistic in the reference run.

c. Comparison with observations and other model studies

CAM-Oslo has already been carefully validated in terms of warm cloud microphysical and radiative properties. In Storelvmo et al. (2006a) and Storelvmo et al. (2006b) critical parameters for the AIE of warm clouds were compared to satellite data, and found to agree

reasonably well with the observations. In Penner et al. (2006) CAM-Oslo was also compared to two other GCMs in an extensive series of experiments investigating aerosol influence on warm clouds. Hence, in this paper we would like to focus on comparing cold cloud properties to observations (when available) and to results from other comparable model studies. By comparing modeled cloud fraction (CFR), IWP and ice crystal number concentrations, an indication of the soundness of the new framework is obtained.

Compared to satellite observations of CFR obtained from the MODIS (Moderate Resolution Imaging Spectroradiometer, <http://modis-atmos.gsfc.nasa.gov>) instrument onboard the Terra satellite, the new framework (here represented by simulation AIE_ref) represents a significant improvement over AIE_liq (Figure 3 a and b). The global average compares fairly well with that from MODIS (64.3% and 65.0%, respectively), while AIE_liq (Figure 3 c) yields an underestimate (60.5%). In particular, the comparison at mid/high latitudes is significantly improved after the implementation of the new framework, indicating that it is in fact the more realistic treatment of ice cloud formation that has led to the improvement. Unfortunately, reliable satellite estimates of IWP are difficult to retrieve (Zhao and Weng, 2002). GCM estimates of IWP vary by one order of magnitude (Del Genio et al. (1996), Lohmann(2002)) indicating that the modeling community so far had little guidance from observations on this important parameter for radiative transfer calculations. In this study we compare the modeled IWP to that obtained from the International Satellite Cloud Climatology Project (ISCCP). IWP is also available from MODIS, but its IWP retrieval algorithm has contained errors for certain data collections (http://modis-atmos.gsfc.nasa.gov/MOD06_L2/qa.html). Figure 4 a) is a global average IWP from the years 1983-2000 produced by adding the IWP for 9 cloud types as reported by ISCCP. Contributing to the total IWP are cirrus, cirrostratus and deep convective clouds, in addition

to the ice fraction of altostratus, altocumulus, nimbostratus, cumulus, stratocumulus and stratus clouds. For the cirrus, cirrostratus and deep convective clouds, we assume that all cloud water is in the ice phase, as their cloud base is by ISCCP definition above 440hPa. However, in the tropics liquid water may well exist above 440hPa, so for the tropical region ($30^{\circ}\text{S} - 30^{\circ}\text{N}$) we assumed that 1/3 of the total water path is liquid (for cirrus, cirrostratus and deep convective clouds only). The global average for the ISCCP IWP is 26.7 g/m^2 , which is significantly larger than predicted by AIE_liq (Figure 4 c, 8.83 g/m^2) but compares very well with the IWPs predicted by the 4 model setups (AIE_ref and the three sensitivity simulations presented in the next section) with the new framework for aerosol influence on mixed-phase clouds ($23.7\text{-}27.4 \text{ g/m}^2$). Figure 4 b displays the IWP from the AIE_ref simulation (PD case) and shows that the model overestimates IWP at high NH latitudes while there is a slight underestimation in the tropics as compared to the ISCCP data. This indicates that the high IN values at NH mid-latitudes evident in Figure 1a are probably unrealistic, which will be discussed in more detail in Section 4.3. Concerning the underestimation at low latitudes, we suggest that this is mainly caused by the host model physics, as the same problem is present also in AIE_liq (Figure 4 c).

Figure 5 shows the zonal mean ice crystal number concentration (ICNC) as predicted by Equation (4) in simulation AIE_ref (PD emissions). As the IN concentration and the concentration of cloud droplets available for freezing decreases with height, while the freezing efficiency increases with decreasing temperatures (i.e. increasing height), the maximum in ICNC at 600-700 hPa is not surprising. Evident from Figure 5 is also the higher ICNC in NH compared to the southern hemisphere (SH) values. Korolev et al. (2003) reported aircraft measurements of ICNC from 5 different field campaigns, all of which took place within the latitude band $42^{\circ} - 74^{\circ}\text{N}$. For glaciated stratiform clouds with temperatures in

the interval -35°C to 0°C , they found the ICNC to be nearly constant at $2\text{-}5\text{ cm}^{-3}$. For the same latitude band in Figure 5, the simulated ICNC values seem to compare fairly well with these measurements. However, there is an ongoing debate in the scientific community on whether these observed values are artificially high due to the problem of ice crystal shattering at the inlet of the Forward Scattering Spectrometer Probes (FSSP) used for the ICNC measurements presented in Korolev et al. (2003). Until more insight into this matter is available from field campaigns and possibly remote sensing, comparisons should be made with great caution. The discrepancy between observed IN concentrations and observed ice particle concentrations has long been a scientific puzzle (Pruppacher and Klett, 1997), and has been interpreted as an indication of the existence of some unknown ice crystal formation mechanism. Only one such secondary production mechanism (the Hallett-Mossop process) is included in our model simulations, and it does not contribute significantly to ice crystal number with the current parameterization. Parameterizations of other secondary production mechanisms are to our knowledge not yet available. The simulated ICNC are higher than those reported by Lohmann and Diehl (2006), which is not surprising considering the higher total IN concentration in CAM-Oslo than in ECHAM4. Additionally, in CAM-Oslo the majority of the IN are dust aerosols (with higher freezing efficiencies than BC), whereas in ECHAM4 BC is the major contributor to the total IN number. On the other hand, ice crystal concentrations presented here are very similar to those simulated by the ECHAM5-HAM GCM presented in Lohmann et al. (2007). Considering the low IN concentrations measured with Continuous Flow Diffusion Chambers (CFDC) by e.g. Rogers et al. (1998) and DeMott et al. (2003), it is possible that both GCMs overestimate the ice crystal production by primary production mechanisms (i.e. homogeneous and heterogeneous freezing). However, uncertainties associated with measurements using a CFDC are also

relatively large. The fact that such chambers have until now only measured deposition and/or condensation freezing is a problem, as contact freezing can be a lot more efficient than these mechanisms, especially in relatively warm mixed-phase clouds. Additionally, the CFDC cannot capture freezing processes taking more than approximately 10 seconds, which can possibly lead to IN underestimates. Hence, while awaiting more and better in situ measurements of IN and ice crystal concentrations, we note that the framework presented here produces ICNC that are on the upper end of what has been observed so far.

In summary, considering the wide range of uncertainty, the simulated cloud fractions, IWPs and ICNCs compare reasonably with observations, and we therefore conclude that the approach is sound and suitable for the sensitivity studies presented in the following section.

4. Results from sensitivity tests

a. AIE_kao

This sensitivity study is similar to one performed in the ECHAM4 GCM and presented in Lohmann and Diehl (2006). The purpose of the sensitivity study is to find out whether the assumption that all mineral dust particles are montmorillonite is critical for the results. As an additional motivation, it is not obvious that the same sensitivity study will give the same result in two different GCMs with numerous differences in their model physics and dynamics.

It turns out that changing the type of mineral dust particles gives qualitatively similar changes in IWP and LWP (due to anthropogenic aerosols) in CAM-Oslo as in ECHAM4. However,

quantitatively the anthropogenic changes in LWP are significantly smaller in CAM_Oslo than in ECHAM4. This is likely to be due to differences in the aerosol size distributions, the treatment of external versus internal aerosol mixtures, and in the parameterization of autoconversion processes to form precipitation in liquid clouds. Additionally, in ECHAM4 anthropogenic aerosols seem to have a significantly stronger influence on cloud cover than in CAM-Oslo. This is probably partly due to the larger anthropogenic fraction of the total IN concentration in ECHAM4, but possibly also because cloud cover is diagnosed differently in the two GCMs. Also, the implementation of the Bergeron-Findeisen mechanism in ECHAM4 was not as efficient as it is here, because cloud droplets were not evaporated and the vapor not deposited onto ice crystals within the same timestep. Instead the remaining droplets had to freeze or form precipitation size particles in subsequent timesteps. If the Bergeron-Findeisen mechanism is as efficient as in CAM-Oslo, the glaciation aerosol effect is much smaller (Hoose et al., 2007).

In both models, the fact that kaolinite is less efficient as IN than montmorillonite allows the soot IN to become relatively more important than otherwise. Consequently, the effect of replacing montmorillonite by kaolinite is a less positive (ECHAM4) or even more negative (CAM-Oslo) anthropogenic change in LWP, while the difference in cloud ice between the PD simulation and the PI run becomes more positive. However, in CAM-Oslo these two effects seem to cancel when it comes to radiative forcings, and the total AIE is practically the same (-0.10 W/m^2) in this case as in AIE_ref (-0.07 W/m^2). A closer look at the freezing mechanisms in the two cases (not shown) reveals that while the differences in contact freezing are relatively small, immersion freezing is significantly less efficient in the AIE_kao case than in AIE_ref. This is expected, as the difference in freezing efficiency for the two mineral dust types is larger in the immersion freezing mode than for contact freezing

(Diehl et al., 2006). As natural IN are less efficient in this case than in AIE_ref, especially through the immersion mode, anthropogenic IN are allowed to play a relatively more important role in cloud glaciation processes. In this sensitivity study, anthropogenic IN therefore have a larger impact on IWP and LWP than in AIE_ref. However, in terms of the total AIE, assuming that all dust particles consist of kaolinite rather than montmorillonite seems to be of little importance in the current setup of CAM-Oslo.

b. AIE_mono

As already mentioned, the fact that all mineral dust and soot aerosols may act as both immersion and contact IN in AIE_ref probably leads to an overestimated freezing rate. In this set of sensitivity simulations, we assume that if sufficient sulfate is available in a grid box to cover a median mineral dust particle with one monolayer of sulfate, then the mineral dust will act as IN through the immersion mode. Otherwise, the mineral dust particles will act as contact IN. This is a simplified approach where the concentrations of both contact and immersion IN are reduced compared to the reference run, and their relative concentrations will depend on the amount of sulfur available for condensation. As a result, freezing is less efficient in these simulations. Consequently, we see an increase in LWP and a decrease in IWP compared to the reference simulations.

Concerning the anthropogenic change in LWP, we now see a significant aerosol lifetime effect again (as in AIE_liq). Freezing is in fact more efficient in the PI run than in the PD simulation, leading to a negative anthropogenic change in IWP. The reason for this is not that the total IN concentration is higher in the PI run, but rather that the number of contact nuclei is higher because less sulfur is available for the transition from contact to immersion

nuclei to occur. Figures 6 a) and b) show that this is particularly true for Northern Hemisphere (NH) mid-latitudes, where the anthropogenic sulfur concentration has its maximum. In the PD simulation, the number of immersion freezing nuclei is proportionally higher at the same levels where contact nuclei concentrations are reduced. But at these levels, temperatures will often be above the onset temperature for immersion freezing. Hence, the increased immersion IN concentration has no impact there. The anthropogenic change in NCF at the TOA is -0.27 W/m^2 , which is a reduction in absolute value by approximately 45% compared to the AIE_liq case. This is due to a slightly smaller anthropogenic change in LWP and R_{eff} than in AIE_liq, and additionally a reduction in IWP of 0.46 g/m^2 . We can conclude that taking the degree of coating into account for the different freezing modes does alter the anthropogenic aerosol impact on clouds. Nevertheless, accounting for the anthropogenic aerosol effect on freezing mechanisms reduces the magnitude of the AIE also in this case.

c. AIE_dust

As the modal radius of the mineral dust accumulation mode is somewhat smaller in CAM-Oslo ($0.088 \mu\text{m}$) than in many other comparable models (Textor et al., 2006), mineral dust number concentrations are relatively high in our simulations. In order to investigate the importance of the mineral dust number concentration for the results, we have carried out sensitivity simulations with a larger modal radius for the mineral dust accumulation mode than that of the reference run. This corresponds to reducing the mineral dust number concentration by approximately a factor of 10. However, the fact that mineral dust particles now become larger does not affect their freezing efficiency, as the heterogeneous freezing

parameterization is independent of IN sizes. As a consequence, heterogeneous freezing (i.e. the sum of immersion and contact freezing) is less efficient in these simulations than in AIE_ref, as evident in Figure 7 a) and b). Therefore, LWP is higher and IWP is lower here than in AIE_ref (Table 2). Also, the ICNC is lower at all model levels in this simulation than in AIE_ref, the largest relative decrease of $\sim 25\%$ being found at approximately 400 hPa. Another consequence is that the fraction of natural IN is reduced, which is expected to increase the sensitivity to anthropogenic IN. Hence, the larger anthropogenic increase in IWP seen in this sensitivity study compared to AIE_ref is expected. However, we do not see a correspondingly large decrease in the LWP. This is puzzling, but can probably be explained by the fact that total cloud glaciation becomes less frequent as fewer IN are available. As the threshold ice mixing ratio required for the Bergeron-Findeisen process to set in is reached, the ambient air becomes sub-saturated with respect to liquid droplets and they therefore rapidly evaporate. As soon as this non-linear process is initiated, all liquid water is frozen and precipitation formation is likely when the ice crystals grow at the expense of the evaporating cloud droplets. Hence, when the total freezing efficiency is low (as in this case), the anthropogenic contribution to freezing is likely to lead to a large increase in IWP and a small reduction in LWP. However, the total anthropogenic change in LWP is still positive due to the Albrecht effect.

The anthropogenic effect on NCF at the TOA (the AIE, in other words) is -0.18 W/m^2 in this case, which is a reduction in magnitude compared to the AIE_liq simulation by more than 60%. The reduction is mainly due to a positive LW forcing, which should be expected considering the increase in IWP and LWP of 0.52 g/m^2 and 0.68 g/m^2 , respectively.

5. Discussion and future work

We have presented a sensitivity study of the aerosol effect on mixed-phase clouds, and find that this effect represents a warming of the earth-atmosphere system. It counteracts the cooling introduced by the aerosol effect on warm clouds, and reduces the magnitude of the total AIE by 45-90% depending on assumptions of IN characteristics. Although we improved the model performance by introducing aerosol effects on mixed-phase clouds, there is clearly room for improvement. The treatment of cirrus cloud ($T < -40^{\circ}\text{C}$) formation and the aerosol impact thereon is currently treated crudely. Additionally, biogenic aerosol particles are not included in the aerosol life cycle module of CAM-Oslo. These aerosols have until recently been considered to constitute an insignificant fraction of the total aerosol mass (Penner et al., 2001). Hence, little effort has been invested in creating biogenic emission scenarios.

However, new attention was recently drawn to this issue by Jaenicke (2005). Based on the insight provided by e.g. Matthias-Mäser and Jaenicke (1995) and papers pointing out the efficiency of certain biogenic particles as IN (e.g. Schnell and Vali (1996) and Levin and Yankofsky (1983)), a natural continuation of the study presented here would be to include biogenic IN. Currently, we have no evidence that biogenic particle concentrations have changed significantly since preindustrial times, but we firmly believe that modeling a correct natural state is crucial for our ability to simulate anthropogenic perturbations realistically.

As already pointed out by Lohmann and Diehl (2006), more measurements of the mineralogical composition of dust are needed in order to model mixed-phase and cold cloud formation accurately. Ideally, one should know the composition of dust at all locations rather than making assumptions about it. This is true for calculations of the aerosol indirect effects on both warm (Storelvmo et al., 2006a) and cold clouds, and also for direct aerosol effects (Sokolik et al., 2001).

Levin et al. (2005) presented results from a case study, apparently contradicting the largely accepted view that an increase in IN increases freezing and hence precipitation efficiency. However, their findings were primarily valid for convective cloud systems, as Levin et al. (2005) hypothesize that ice crystal production inhibits graupel formation and therefore precipitation formation. So far, aerosol influence on convective clouds has not been accounted for in GCMs, as convective clouds typically occur on scales significantly smaller than those resolved by such models. Hence, this study was carried out for stratiform clouds only, and we still believe that for such clouds an increase in IN will lead to increased freezing and therefore more efficient precipitation release through the ice phase. This is based on the reasoning that additional IN may glaciare clouds which would otherwise remain mainly liquid. In clouds which would glaciare independent of the contribution from additional aerosols, the impact on precipitation is assumed to be small. In fact, the additional IN could then reduce precipitation due to more numerous and therefore smaller ice crystals, as shown by Diehl et al. (2006). However, as IN concentrations are generally orders of magnitudes lower than CCN concentrations, ice crystals in mixed-phase clouds will typically always grow large enough to form precipitation.

Bailey and Hallett (2002) carried out laboratory studies revealing something truly intriguing from a climate change point of view; namely that different IN tend to favor different ice crystal shapes. This brings two of the most challenging questions in the study of mixed-phase clouds together: “What determines the ice crystal shape in an ice cloud?” and “What is the anthropogenic aerosol influence on ice clouds?” Further investigations of the findings presented in Bailey and Hallett (2002) would be an interesting extension to the work presented in this paper. In particular, we would like to answer to the following questions: i) Do different IN nucleate ice crystals with different ice crystal shapes? ii) Do anthropogenic

IN differ significantly from natural IN in this sense? iii) If so, what is the climatic effect of this anthropogenic ice crystal shape change?

ACKNOWLEDGEMENTS

The work presented in this paper has been supported by the Norwegian Research Council through the NORCLIM project (grant no. 178246). Furthermore, this work has received support of the Norwegian Research Council's program for Supercomputing through a grant of computer time. We are grateful to Alf Kirkevåg, Øyvind Seland and Trond Iversen for their important roles in the CAM-Oslo model development. We are also grateful to Steven Ghan at the Pacific Northwest National Laboratory for making his droplet activation scheme available and for help in implementing it in CAM-Oslo. Finally, we are thankful to two anonymous reviewers whose comments led to significant improvements of the paper.

References

Abdul- Razzak, H. and S. Ghan, 2000: A parameterization of aerosol activation, 2. Multiple aerosol type. *J. Geophys. Res.*, **105**, 6837-6844.

Albrecht, B. A., 1989: Aerosols, cloud microphysics, and fractional cloudiness. *Science*, **245**, 1227-1230.

Andreae, M. O., C. D. Jones and P. M. Cox, 2005: Strong present-day aerosol cooling implies a hot future. *Science*, **435**, 1187-1190.

Bailey, M. and J. Hallett, 2002: Nucleation effects on the habit of vapour grown ice crystals from -18°C to -42°C. *Q. J. R. Meteorol. Soc.*, **128**, 1461-1483.

Boudala, F. S., G. A. Isaac, Q. Fu and S. G. Cober, 2002: Parameterization of effective ice particle size for high-latitude clouds. *Int. J. Climatol.*, **22**, 1267-1284.

Chen, Y, S. M. Kreidenweis, L. M. McInnes, D. C. Rogers and P. J. DeMott, 1998: Single particle analyses of ice nucleating aerosols in the upper troposphere and lower stratosphere. *Geophys. Res. Lett.*, **25**, 1391-1394.

Collins, W. D., 2001: Parameterization of generalized cloud overlap for radiative calculations in general circulation models. *J. Atmos. Sci.*, **58**, 3224-3242.

Del Genio, A., M.-S. Yao, W. Kovari and L.W. Lo, 1996: A prognostic cloud water parameterization for global climate models. *J. Climate*, **9**, 270-304.

DeMott, P. J., D. C. Rogers and S. Kreidenweis, 1997: The susceptibility of ice formation in upper tropospheric clouds to insoluble aerosol components. *J. Geophys. Res.*, **102**, 19575-19584.

DeMott, P. J., D. J. Cziczo, A. J. Prenni, D. M. Murphy, S. M. Kreidenweis, D. S. Thomson, R. Borys and D. C. Rogers, 2003: Measurements of the concentration and composition of nuclei for cirrus formation. *Proc. Natl. Acad. Sci. USA*, **100**, 14655-14660.

Diehl, K. and S. Wurzler, 2004: Heterogeneous drop freezing in the immersion mode: Model calculations considering soluble and insoluble particles in the drops. *J. Atmos. Sci.*, **61**, 2063 – 2072.

Diehl, K., M. Simmel and S. Wurzler, 2006: Numerical simulations on the impact of aerosol properties and freezing modes on the glaciation, microphysics and dynamics of convective clouds. *J. Geophys. Res.*, **111**, doi: 10.1029/2005JD005884.

Dymarska, M. B., J. Murray, L. Sun, M. L. Eastwood, D. A. Knopf and A. K. Bertram, 2006: Deposition ice nucleation on soot at temperatures relevant for the lower troposphere. *J. Geophys. Res.*, **111**, doi: 10.1029/2005JD006627.

Ebert, E. E. and J. A. Curry, 1992: A parameterization of ice cloud radiative properties for climate models. *J. Geophys. Res.*, **97**, 3831-3836.

Ghan, S. J., N. S. Laulainen, R. C. Easter, R. Wagener, S. Nemesure, E. G. Chapman, Y. Zhang and L. R. Leung, 2001: Evaluation of aerosol direct radiative forcing in MIRAGE. *J. Geophys. Res.*, **106**, 5295-5316.

Gorbunov, B., A. Baklanov, N. Kakutkina, H. L. Windsor and R. Toumi, 2001: Ice nucleation on soot particles. *J. Aerosol Sci.*, **32**, 199-215.

Hallett, J. and S. C. Mossop, 1974: Production of secondary ice particles during the riming process. *Nature*, **249**, 26-28.

Hansen, J., M. Sato, L. Nazarenko, R. Ruedy, A. Lacis, D. Koch, I. Tegen, T. Hall, D. Shindell, B. Santer, P. Stone, T. Novakov, L. Thomason, R. Wang, Y. Wang, D. Jacob, S. Hollandsworth, L. Bishop, J. Logan, A. Thompson, R. Stolarski, J. Lean, R. Willson, S. Levitus, J. Antonov, N. Rayner, D. Parker and J. Christy, 2002: Climate forcings in Goddard Institute for Space Studies SI2000 simulations. *J. Geophys. Res.*, **107**, doi:10.1029/2001JD001143.

Heymsfield, A. J., L. M. Miloshevich, C. Twohy, G. Sachse and S. Oltmans, 1998: Upper tropospheric relative humidity observations and implications for cirrus ice nucleation. *Geophys. Res. Lett.*, **25**, 1343-1346.

Hoose, C., U. Lohmann, R. Erdin and I. Tegen, 2007: Global Influence of Dust Mineralogical Composition on Heterogeneous Ice Nucleation. *Submitted to Environ. Res. Lett.*

Hung, H.-M., A. Malinowski and S. T. Martin, 2003: Kinetics of heterogeneous ice nucleation on the surfaces of mineral dust cores inserted into aqueous ammonium sulfate particles. *J. Phys. Chem.*, **A107**, 1296-1306.

Intrieri, J. M., M. D. Shupe, T. Uttal and B. J. McCarty, 2002: An annual cycle of Arctic cloud characteristics observed by radar and lidar at SHEBA. *J. Geophys. Res.*, **107**, doi:10.1029/2000JC000423.

Ivanova, D., D. L. Mitchell, W. P. Arnott and M. Poellot, 2001: A GCM parameterization for bimodal size spectra and ice mass removal rates in mid-latitude cirrus clouds. *Atm. Res.*, **59-60**, 89-113.

Iversen, T. and Ø. Seland, 2002: A scheme for process-tagged SO₄ and BC aerosols in NCAR CCM3. Validation and sensitivity to cloud processes. *J. Geophys. Res.*, **107 (D24)**, 4751, 10.1029/2001JD000885.

Jaenicke, R., 2005: Abundance of Cellular Material and Proteins in the Atmosphere. *Science*, **308**, 73.

Jensen, E. J., O. B. Toon, D. L. Westphal, S. Kinne, A. J. Heymsfield, 1994: Microphysical modeling of cirrus 1. Comparison with 1986 FIRE IFO measurements. *J. Geophys. Res.*, **99(D5)**, 10421-10442, 10.1029/93JD02334.

Kärcher, B. and U. Lohmann, 2002: A parameterization of cirrus cloud formation: Homogeneous freezing of supercooled clouds. *J. Geophys. Res.*, **107**, 4010, doi: 10.1029/2001JD000470.

Kärcher, B., J. Hendricks and U. Lohmann, 2006: Physically based parameterization of cirrus cloud formation for use in global atmospheric models. *J. Geophys. Res.*, **111**, D01205, doi: 10.1029/2005JD006219.

Kerr, R. A., 2005: How Hot Will The Greenhouse Be? *Science*, **309**, 100.

Kiehl, J. T., J. J. Hack and B. P. Briegleb, 1994: The simulated Earth radiation budget of the National Center for Atmospheric Research community climate model CCM2 and comparisons with the Earth Radiation Budget Experiment (ERBE). *J. Geophys. Res.*, **99(D10)**, 20815-20828, 10.1029/94JD0117.

Kirkevåg, A. and T. Iversen, 2002: Global direct radiative forcing by process-parameterized aerosol optical properties. *J. Geophys. Res.*, **107(D20)**, 4433, doi: 10.1029/2001JD000886.

Kirkevåg, A., T. Iversen, Ø. Seland and J.E. Kristjánsson, 2005: Revised schemes for aerosol optical parameters and cloud condensation nuclei. *Institute Report Series, No. 128*.

Department of Geosciences, University of Oslo.

Korolev, A., S. G. Cober, W. Strapp and J. Hallet, 2003: Microphysical characterization of mixed-phase clouds. *Quart. J. Roy. Meteor. Soc.*, **129**, 39-65.

Korolev, A. and G. A. Isaac, 2006: Relative Humidity in Liquid, Mixed Phase and Ice Clouds. *J. Atm. Sci.*, **63**, 2865-2880.

Kristjánsson, J. E., J. M. Edwards, and D. L. Mitchell, 2000: Impact of a new scheme for optical properties of ice crystals on climates of two GCMs. *J. Geophys. Res.*, **105**, 10063-10079.

Kristjánsson, J. E., 2002: Studies of the aerosol indirect effect from sulfate and black carbon aerosols. *J. Geophys. Res.*, **107**, 4246, doi:10.1029/2001JD000887.

Levin, Z. and S.A. Yankofsky, 1983: Contact versus immersion freezing of freely suspended droplets by bacterial ice nuclei. *J. Clim. Appl. Meteorol.*, **22**, 1964-1966.

Levin, Z., Teller, A., Ganor, E. and Yin, Y., 2005: On the interactions of mineral dust, sea salt particles, and clouds: A measurement and modeling study from the Mediterranean Israeli Dust Experiment campaign. *J. Geophys. Res.*, **110**, doi: 10.1029/2005JD005810.

Levkov, L. B., B. Rockel, H. Kapitzka and E. Raschke, 1992: 3D mesoscale numerical studies of cirrus and stratus clouds by their time and space evolution. *Beitr. Phys. Atmos.*, **65**, 35-58.

Lohmann, U., J. Feichter, J. E. Penner and R. Leaitch, 2000: Indirect effect of sulfate and carbonaceous aerosols: A mechanistic treatment. *J. Geophys. Res.*, **105**, 12193-12206.

Lohmann, U., 2002: Possible aerosol effects on ice clouds via contact nucleation. *J. Atmos. Sci.*, **59**, 647-656.

Lohmann, U. and B. Kärcher, 2002: First interactive simulations of cirrus clouds formed by homogeneous freezing in the ECHAM general circulation model. *J. Geophys. Res.*, **107**, doi: 10.1029/2001JD000767.

Lohmann, U. and J. Feichter, 2005: Global indirect aerosol effects: a review. *Atmos. Chem. Phys.*, **5**, 715-737.

Lohmann, U. and K. Diehl, 2006: Sensitivity Studies of the Importance of Dust Ice Nuclei for the Indirect Aerosol Effect on Stratiform Mixed-Phase Clouds. *J. Atmos. Sci.*, **63**, 968-982.

Lohmann, U., P. Stier, C. Hoose, S. Ferrachat, E. Roeckner and J. Zhang, 2007: Cloud microphysics and aerosol indirect effects in the global climate model ECHAM5-HAM. *Atm. Chem. Phys.*, **7**, 3385-3398.

Matthias-Maser, S and R. Jaenicke, 1995: Size distributions of primary biological aerosols particles with radii $> 0.2 \mu\text{m}$. *Atmos. Res.*, **39(4)**, 279-286.

McFarquhar, G. M. and A. J. Heymsfield, 1996: Microphysical Characteristics of Three Anvils sampled during the Central Equatorial Pacific Experiment. *J. Atmos. Sci.*, **53**, 2401-2423.

Menon, S., A. D. Del Genio, D. Koch and G. Tselioudis, 2002: GCM Simulations of the Aerosol Indirect Effect: Sensitivity to Cloud Parameterization and Aerosol Burden, *J. Atmos. Sci.*, **59**, 692-713.

Ou, S.-C., and K.-N. Liou, 1995: Ice microphysics and climatic temperature feedback, *Atmos. Res.*, **35**, 127-138.

Penner, J. E., Andreae, M., Annegarn, H., Barrie, L., Feichter, J., Hegg, D., Jayaraman, A., Leaicht, R., Murphy, D., Nganga, J. and Pitari, G., 2001: Aerosols, their direct and indirect effects, Chapter 5 (pp. 289-348) in: *Climate change 2001: The scientific basis. Contribution of working group I to the Third Assessment Report of the Intergovernmental Panel on Climate Change. Cambridge University Press.*

Penner, J., J. Quaas, T. Storelvmo, T. Takemura, O. Boucher, H. Guo, A. Kirkevåg, J. E. Kristjánsson and Ø. Seland, 2006: Model intercomparison of the aerosol indirect effect. *Atmos. Chem Phys.*, **6**, 3391 -3405, SRef-ID: 1680-7324/acp/2006-6-3391.

Peter, T., Marcolli, C., Spichtinger, P., Corti, T., Baker, M. B. and T. Koop, 2006: When dry air is too humid. *Science*, **5804(314)**, 1399-1402.

Pitter, R.L. and Pruppacher, H. R., 1973: Wind tunnel investigation of freezing of small water drops falling at terminal velocity in air. *Quart. J. Roy. Meteor. Soc.*, **99**, 540-550.

Pruppacher, H. R. and J. D. Klett, 1997: Microphysics of Clouds and Precipitation. *Kluwer Acad., Norwell, Mass.*

Quaas, J., O. Boucher and U. Lohmann, 2006: Constraining the total aerosol indirect effect in the LMDZ and ECHAM4 GCMs using MODIS satellite data. *Atm. Chem. Phys.*, **6**, 947-955.

Rasch, P. J. and J. E. Kristjánsson, 1998: A comparison of the CCM3 model climate using diagnosed and predicted condensate parameterizations. *J. Climate*, **11**, 1587-1614..

Rogers, D. C., P. J. DeMott, S. M. Kreidenweis and Yalei Chen, 1998: Measurements of ice nucleating aerosols during SUCCESS. *Geophys. Res. Lett.*, **25**, 1383-1386.

Rotstayn, L. D. and Y. Liu, 2003: Sensitivity of the First Aerosol Indirect Effect to an increase of Cloud Droplet Spectral Dispersion with Droplet Number Concentration. *J. Clim.*, **16**, 3476-3481.

Sassen, K., P. J. DeMott, J. M. Prospero and M. R. Poellot, 2003: Saharan dust storms an

indirect aerosol effects on clouds Forcing: CRYSTAL-FACE results. *Geophys. Res. Lett.*, **30**, doi: 10.1029/2003GL017371.

Sax, R. I. and P. Goldsmith, 1927: Nucleation of water drops by Brownian contact with AgI and other aerosols. *Quart. J. R. Met. Soc.*, **98**, 60-72.

Schnell, R. C., and G. Vali, 1976: Biogenic Ice Nuclei: Part I. Terrestrial and Marine Sources. *J. Atm. Sci.*, **33**, 1554-1564.

Slingo, A., 1989: A GCM parameterization for the shortwave properties of water clouds. *J. Atmos. Sci.*, **46**, 1419-1427.

Sokolik, I. N., D. M. Winker, G. Bergametti, D. A. Gillette, G. Carmichael, Y. J. Kaufman, L. Gomes, L. Schuetz and J. E. Penner, 2001: Introduction to special section: Outstanding problems in quantifying the radiative impacts of mineral dust. *J. Geophys. Res.*, **106**, 18015-18027.

Storelvmo, T., J. E. Kristjánsson, S. J. Ghan, A. Kirkevåg, Ø. Seland and T. Iversen, 2006a: Predicting cloud droplet number concentration in CAM-Oslo. *J. Geophys. Res.*, **111**, doi:10.1029/2005JD006300.

Storelvmo, T., J. E. Kristjánsson, G. Myhre, M. Johnsrud and F. Stordal, 2006b: Combined Observational and Modeling Based Study of the aerosol indirect effect. *Atm. Chem. Phys.*, **6**, 3583-3601, SRef-ID: 1680-7324/acp/2006-6-3583.

Takemura, T., T. Nozawa, S. Emori, T. Y. Nakajima and T. Nakajima, 2005: Simulation of climate response to aerosol direct and indirect effects with aerosol transport-radiation model. *J. Geophys. Res.*, **110**, doi:10.1029/2004JD00502.

Textor, C., M. Schultz, S. Guibert, S. Kinne, Y. Balkanski, S. Bauer, T. Berntsen, T. Berglen, O. Boucher, M. Chin, F. Dentener, T. Diehl, R. Easter, H. Feichter, D. Fillmore, S. Ghan, P. Ginoux, S. Gong, A. Grini, J. Hendricks, L. Horowitz, P. Huang, I. Isaksen, T. Iversen, S. Kloster, D. Koch, A. Kirkevåg, J. E. Kristjánsson, M. Krol, A. Lauer, J. F. Lamerque, X. Liu, V. Montanaro, G. Myhre, J. Penner, G. Pitari, S. Reddy, Ø. Seland, P. Stier, T. Takemura and X. Tie, 2005: Analysis and quantification of the diversities of aerosol life cycles within AeroCom. *Atm. Chem. Phys.*, **6**, 1777-1813.

Twomey, S., 1977: The influence of pollution on shortwave albedo of clouds. *J. Atmos. Sci.*, **34**, 1149-115.

Vali, G., 1985: Atmospheric ice nucleation – a review. *J. Rech. Atmos.*, **19**, 105-115.

Zhang, G. J. and N. A. McFarlane, 1995: Sensitivity of Climate simulations to the parameterizations of cumulus convection in the Canadian Climate Centre general circulation model. *Atmosphere-Ocean*, **33**, 407–446.

Zhao, L. and F. Weng, 2002: Retrieval of Ice Cloud Parameters Using the Advanced Microwave Sounding Unit. *J. Appl. Met.*, **41**, 384-395.

Table 1: Short descriptions of the five simulations carried out in this study: AIE_ref is the reference simulation, AIE_liq is without aerosol effects on freezing, AIE_kao, AIE_mono and AIE_dust are three sensitivity simulations.

SIMULATION	DESCRIPTION
AIE_ref	Simulation with aerosol effects on both warm and mixed-phase clouds included. Aerosol effects on freezing based on the assumption that all BC and mineral dust aerosols (when multiplied by a freezing efficiency) may act as both immersion and contact freezing nuclei. All dust is assumed to be montmorillonite.
AIE_liq	Simulation with only aerosol effects on warm clouds included. Ice fraction in clouds is determined based on temperature only, increasing linearly from 0 at 0°C to 1 at -20°C.
AIE_kao	Similar to AIE_ref, except that all mineral dust particles are assumed to consist of kaolinite rather than montmorillonite.
AIE_mono	Simulation where BC and mineral dust aerosols act either as contact or immersion freezing nuclei. If coated with soluble material exceeding one monolayer, they are assumed to be immersion freezing nuclei. Otherwise they are assumed to be contact freezing nuclei.
AIE_dust	Similar to AIE_ref, except that the modal radius of the mineral dust accumulation mode is increased from 0.088 μm to 0.2 μm , reducing the mineral dust number concentration by one order of magnitude everywhere except in deserts.

Table 2: Cloud microphysical and radiative properties in the reference simulation (AIE_ref), a simulation without aerosol effects on freezing (AIE_liq), and three sensitivity simulations (AIE_kao, AIE_mono, AIE_dust). The absolute values are given for PD aerosol emissions, along with changes in these values due to anthropogenic aerosol emissions, calculated as the difference in the respective parameters between PD and PI simulations, PD-PI. (SWCF = Short Wave Cloud Forcing; LWCF = Long Wave Cloud Forcing; LWP = Liquid Water Path; IWP = Ice Water Path; R_{eff} = Effective droplet radius; TCC = Total Cloud Cover, NCF = Net Cloud Forcing).

	AIE_liq	AIE_ref	AIE_kao	AIE_mono	AIE_dust
SWCF (W/m^2)	-48.1	-54.1	-54.7	-55.8	-54.7
Δ SWCF (W/m^2)	-0.36	-0.11	-0.06	-0.17	-0.30
LWCF (W/m^2)	29.2	32.4	32.2	32.2	32.3
Δ LWCF (W/m^2)	-0.13	0.04	-0.04	-0.10	0.12
LWP (g/m^2)	62.2	91.8	103.1	105.3	99.2
Δ LWP (g/m^2)	0.87	-0.07	-0.32	0.64	0.68
IWP (g/m^2)	8.83	27.4	23.4	23.7	24.4
Δ IWP (g/m^2)	-0.04	0.20	0.36	-0.46	0.52
R_{eff} (μm)	13.2	13.2	13.3	13.3	13.2
ΔR_{eff} (μm)	-0.44	-0.33	-0.32	-0.43	-0.41
TCC (%)	60.5	64.8	64.8	65.1	64.8
Δ TCC (%)	-0.09	0.19	0.01	-0.06	0.12
Δ NCF (W/m^2)	-0.49	-0.07	-0.10	-0.27	-0.18

List of Figures

Figure 1: Zonal means for the two aerosol species in CAM-Oslo suitable for ice nucleation: a) Dust aerosol concentration (similar in PD and PI simulations). b) BC aerosol concentration for PD aerosol emissions. c) BC aerosol concentration for PI aerosol emissions.

Figure 2: Global mean cloud ice fraction averaged over 5 years as calculated by the new framework for aerosol effects on ice clouds (solid line) and that of the original CAM2.0.1 method (dashed line)

Figure 3: Cloud fractions from a) MODIS, b) simulation AIE_ref and c) simulation AIE_liq

Figure 4: Ice Water Path (IWP) from: a) the ISCCP data set, b) the AIE_ref simulation, c) the AIE_liq simulation.

Figure 5: Ice crystal number concentration (ICNC) calculated by the new continuity equation for this quantity in the reference simulation (AIE_ref).

Figure 6: Rate of ice crystal production through contact freezing for the AIE_mono sensitivity test; a) PD simulation and b) PI simulation

Figure 7: Rate of ice crystal production through heterogeneous freezing processes in a) AIE_ref and b) AIE_dust, both from PD simulations.

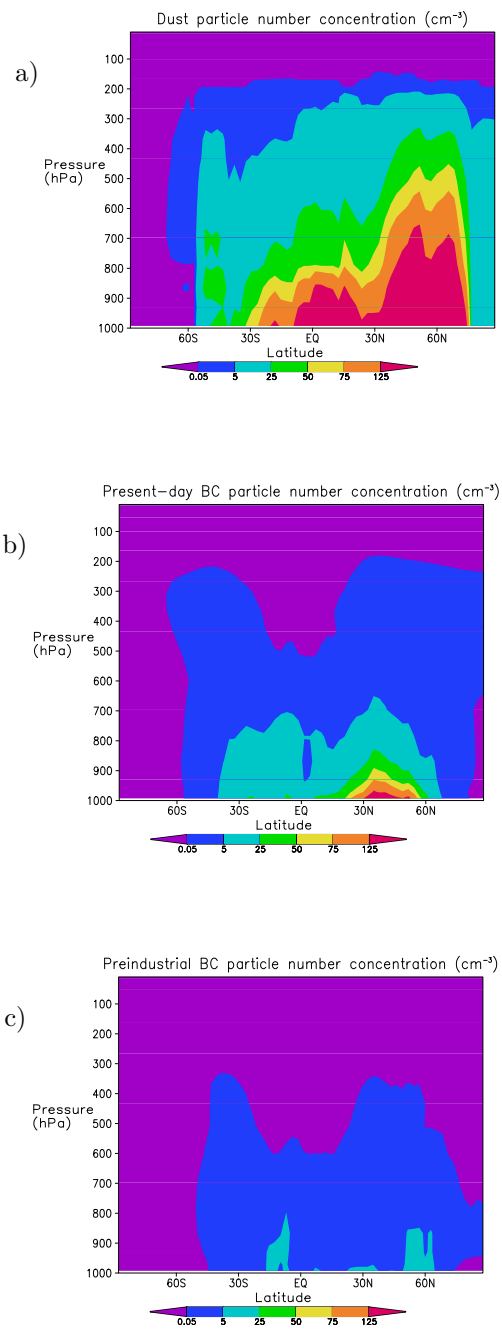


Figure 1: Zonal means for the two aerosol species in CAM-Oslo suitable for ice nucleation: a) Dust aerosol concentration (similar in PD and PI simulations). b) BC aerosol concentration for PD aerosol emissions. c) BC aerosol concentration for PI aerosol emissions.

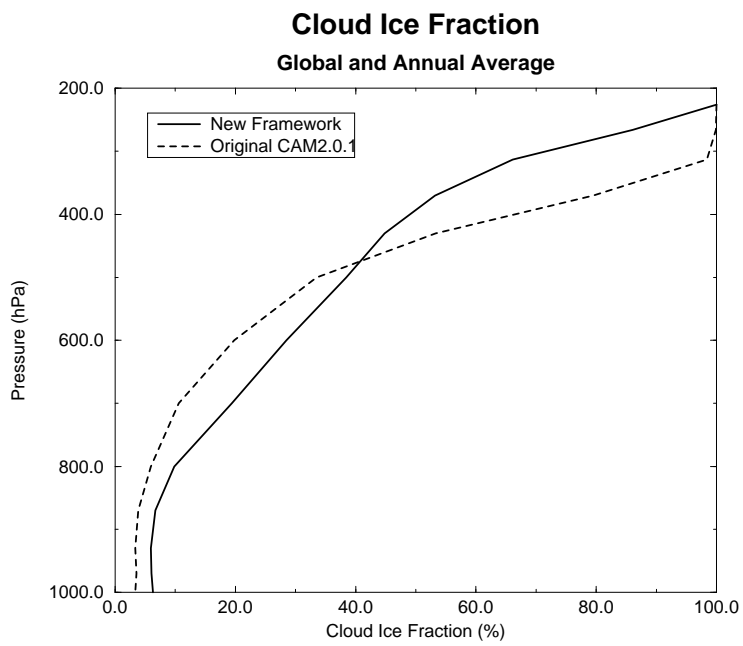


Figure 2: Global mean cloud ice fraction averaged over 5 years as calculated by the new framework for aerosol effects on ice clouds (solid line) and that of the original CAM2.0.1 method (dashed line).

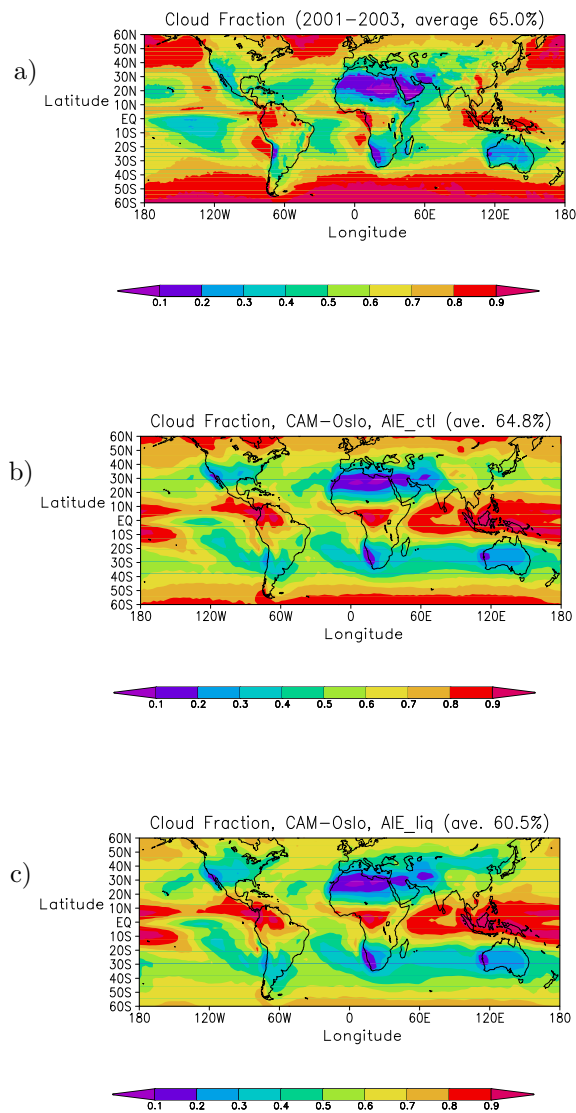


Figure 3: Cloud fractions from a) MODIS, b) simulation AIE_ctl and c) simulation AIE_liq.

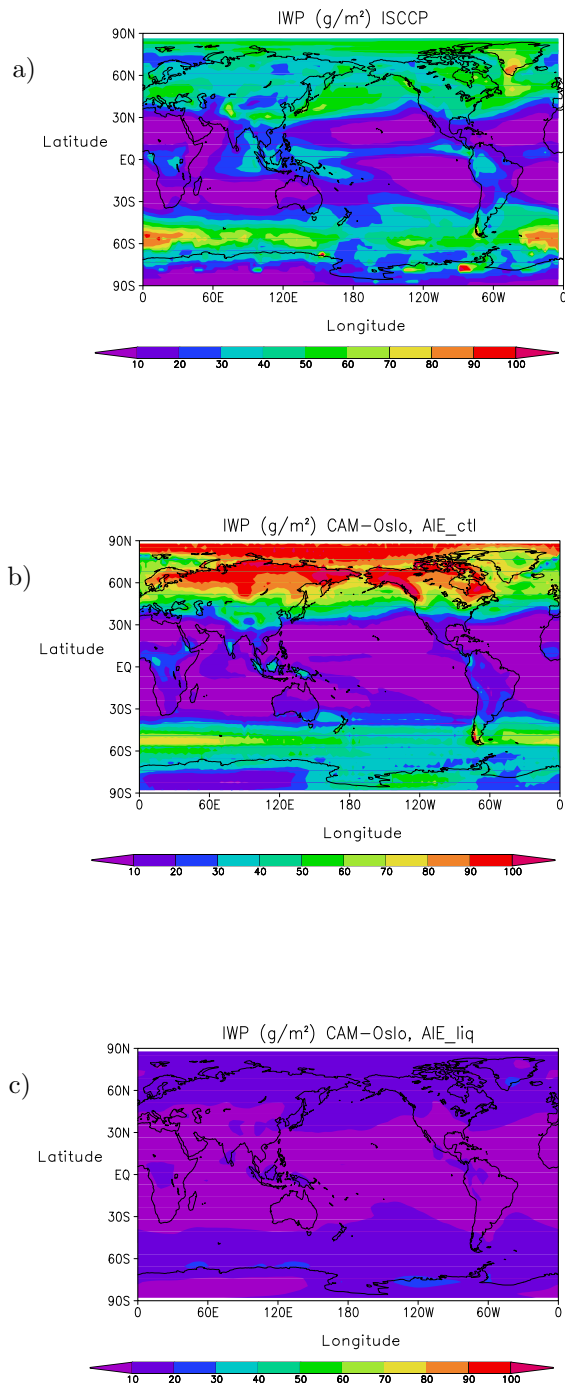


Figure 4: Ice Water Path (IWP) from a) the ISCCP data set, b) simulation AIE_ctl and c) simulation AIE_liq.

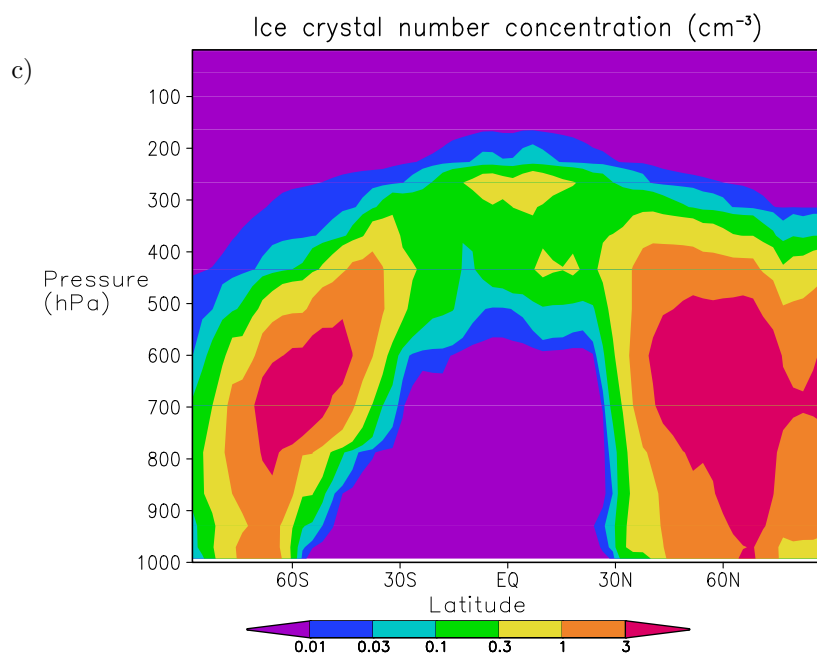


Figure 5: Ice crystal number concentration (ICNC) calculated by the new continuity equation for this quantity in the control simulation (AIE_ctl).

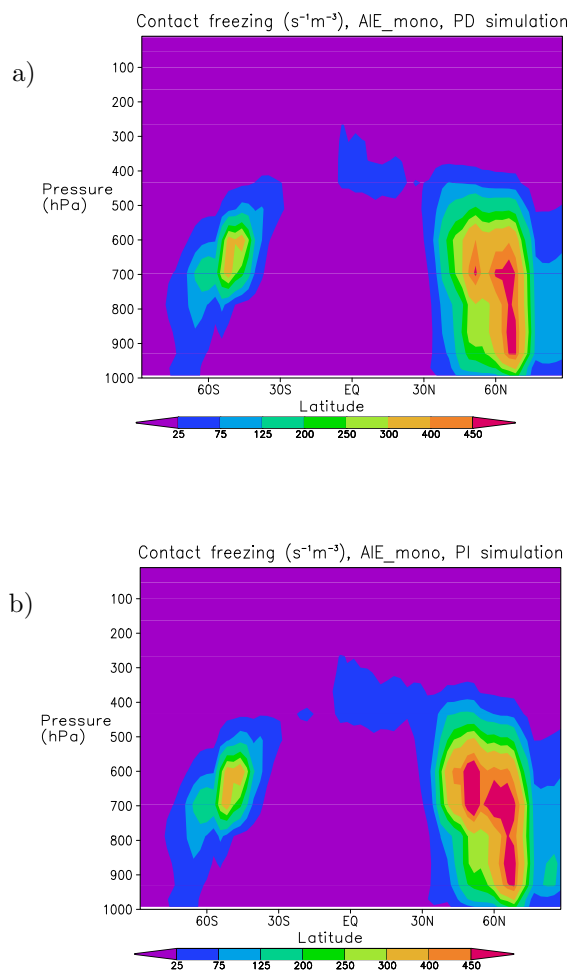


Figure 6: Rate of ice crystal production through contact freezing for the AIE_mono sensitivity test; a) PD simulation, b) PI simulation.

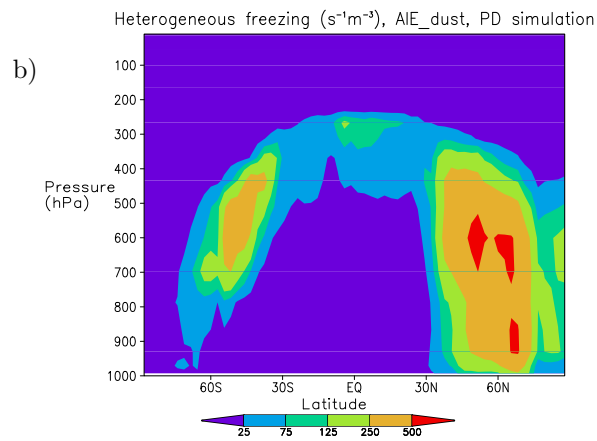
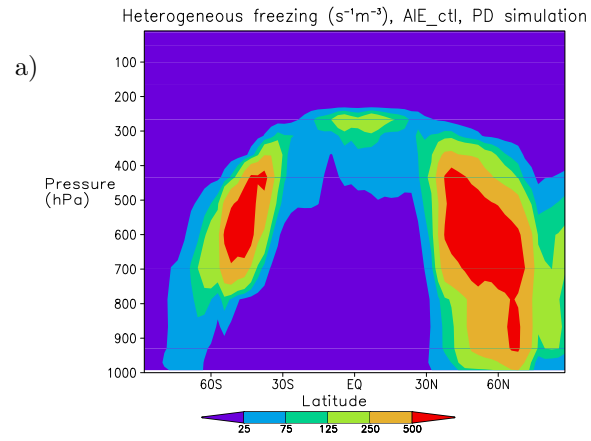


Figure 7: Rate of ice crystal production through heterogeneous freezing processes in a) AIE_ctl and b) AIE_dust, both from PD simulations.